

Contrast and Clustering: Learning Neighborhood Pair Representation for Source-free Domain Adaptation

Yuqi Chen¹, Xiangbin Zhu¹ and Yonggang Li² and Yingjian Li¹ and Yuanwang Wei² and Haojie Fang³

¹Zhejiang Normal University

²Jiaying University

³Zhejiang Sci-Tech University

mochizuki@zjnu.edu.cn, zhuxb@zjnu.cn, liyonggang@zjxu.edu.cn, liyingjian.li@163.com, yuanwang_wei@zjxu.edu.cn, 18868901971@163.com

Abstract

Domain adaptation has attracted a great deal of attention in the machine learning community, but it requires access to source data, which often raises concerns about data privacy. We are thus motivated to address these issues and propose a simple yet efficient method. This work treats domain adaptation as an unsupervised clustering problem and trains the target model without access to the source data. Specifically, we propose a loss function called contrast and clustering (CaC), where a positive pair term pulls neighbors belonging to the same class together in the feature space to form clusters, while a negative pair term pushes samples of different classes apart. In addition, extended neighbors are taken into account by querying the nearest neighbor indexes in the memory bank to mine for more valuable negative pairs. Extensive experiments on three common benchmarks, VisDA, Office-Home and Office-31, demonstrate that our method achieves state-of-the-art performance. The code will be made publicly available at <https://github.com/yukilulu/CaC>.

1 Introduction

The appetite for massive labeled training data has been successfully addressed in unsupervised learning. Significant degradation will occur if the data distributions in the source and target domains are very different, which is formally denoted as domain/distribution shift. To tackle the generalization of the model to unseen domains, domain adaptation (DA) methods [Huang *et al.*, 2022; Lin *et al.*, 2022] based on cotraining of source and target data are conceptually simple, i.e., transferring learned knowledge from the source domain to the target domain. However, with increasing concern about data privacy and data transfer bottlenecks of large datasets, it is extremely unrealistic to require the coexistence of source and target data. In this privacy-preserving scenario, previous unsupervised DA methods could not be deployed, and thus, source-free domain adaptation (SFDA) has emerged over time. The purpose of SFDA is to obtain high performance in an unlabeled target domain, where the source data

are not available during the target adaptation process. Existing SFDA methods [Roy *et al.*, 2022; Hou and Zheng, 2021; Qiu *et al.*, 2021] try to better learn domain invariant/variant representations; however, these methods either require an auxiliary network [Li *et al.*, 2020; Xia *et al.*, 2021], or complex extra data processing is used [Lee *et al.*, 2022; Kundu *et al.*, 2022]. Other methods [Liang *et al.*, 2021; Wang *et al.*, 2022] are negatively affected by noisy labels may predict incorrect target pseudolabels.

The above observation motivates us to tackle the data shift issue in SFDA. There are two obstacles: one is the unlabeled target data, and the other is that the source data cannot be obtained directly, relying only on the pretrained source model. Based on the fact that classes are shared between the source and target domains under closed set DA [You *et al.*, 2019; Kundu *et al.*, 2020], it is reasonable to assume that the pretrained source model can learn the class representation of the target data. Therefore, even if the source and target data are shifted in the feature space, the features extracted by the source model on the target data can form rough clusters through intrinsic class representation information (e.g., husky should never be classified as parrot), where the softmax output of similar features should be highly consistent.

To achieve without the need for specialized source training or changing the model structure, we expect to use the knowledge learned from the source model for self-supervised learning on unlabeled target data. Inspired by recent contrastive learning [He *et al.*, 2020; Oord *et al.*, 2018] (which, as the name implies, learns feature representations by comparing positive and negative samples), it is shown that the data itself provide supervision for network learning. Unlike previous methods that only add samples or change the definition of positive pairs, we first define two probability functions, the probability of having the same class as their positive and negative samples. Then, our method, named Contrast and Clustering (CaC), is obtained by taking the negative logarithm of these two probability functions. As illustrated in the Figure 1, we define the nearest neighbor samples as positive pairs and the neighbors of other samples as negative pairs to achieve contrastive clustering with more sample pairs. Simultaneously, considering that harder negative pairs [Kalantidis *et al.*, 2020; Mitrovic *et al.*, 2020] facilitate better and faster learning, we introduce extended neighbors to exclude similar samples in the

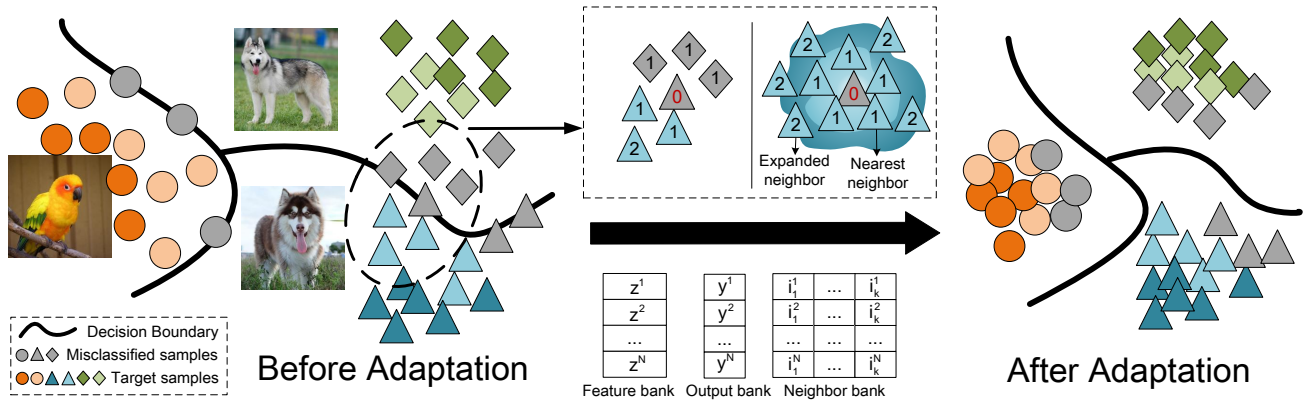


Figure 1: An overview of the proposed method. CaC learns features of the unlabeled target data from pretrained source network, and then these prototype features are used for unsupervised learning clustering.

negative pool to extract more valuable negative pairs. These extended neighbors are computationally costless because they are obtained by querying the nearest neighbor index in the memory bank. In practice, negative pair term is not always effective. We find that the contrastive self-supervised performance degrades on the class-imbalanced dataset, and we address this problem by recursively decoupling positive and negative samples[Yeh *et al.*, 2022] during training. The experimental results show that the proposed method is sufficiently effective on three source-free domain adaptation benchmarks, and it outperforms recent state-of-the-art methods on the challenging dataset VisDA.

The primary contributions of this work are as follows:

1. We propose a contrastive clustering loss function for SFDA, which uses nearest neighbors to learn more information for intraclass compactness and interclass separation in a self-supervised manner.
2. Extended neighbors are taken into account to mine more valuable negative pairs, and these extended neighbors are obtained by querying the nearest neighbor indexes in the memory bank without incurring additional computational cost.
3. The experimental results on three datasets demonstrate the effectiveness and state-of-the-art of our method.

2 Related Work

Domain Adaptation Domain adaptation attempts to learn a powerful classifier from the source domain to the target domain. To generate similar feature distributions from different domain data, the early adversarial adaptation method [Ganin *et al.*, 2016] combines domain adaptation with a two-player game similar to generative adversarial networks. CDAN[Long *et al.*, 2018] extends the conditional adversarial mechanism to enable discriminative and transferable domain adaptation. SRDC[Tang *et al.*, 2020] directly reveals intrinsic target discrimination by discriminative clustering of target data. CaCo [Huang *et al.*, 2022] introduces contrastive learning, encouraging networks to learn representations with different categories

but different domains. However, the source data are not directly available in practice due to privacy issues, making these methods unapplicable.

Source-Free Domain Adaptation The abovementioned normal domain adaptation methods need to access source domain data during target adaptation. Recently, many methods have emerged to tackle source-free domain adaptation(SFDA), which has no way of accessing source data. SHOT[Liang *et al.*, 2020] tunes the source classifier to encourage interclass feature clustering by maximizing mutual information and pseudolabeling. 3C-GAN[Li *et al.*, 2020] is based on conditional GAN to provide supervised adaptation by regularizing the source domain information gradually. NRC[Yang *et al.*, 2021] proposes neighborhood clustering, which performs predictive consistency among local neighborhoods. CPGA[Qiu *et al.*, 2021] proposes a contrastive prototype generation strategy to generate feature prototypes for each class. U-SFAN[Roy *et al.*, 2022] accounts for uncertainty by placing priors on the parameters of the source model. DIPE[Wang *et al.*, 2022] captures such domain-invariant parameters in the source model to generate domain-invariant representations.

Contrastive Learning Contrast learning is a type of self-supervised learning, in which knowledge is learned by constructing pair samples: similar data (positive samples) and dissimilar data (negative samples). There are various ways to construct positive and negative sample pairs. [Ye *et al.*, 2019; Chen *et al.*, 2020] construct pair samples from the current minibatch, where the enhanced samples are positive pair. [Tian *et al.*, 2020] treat data from different views of the same scene as positive pairs and data from different scenes as negative pairs. NNCLR[Dwivedi *et al.*, 2021] uses data augmentation and its nearest neighbors in the memory bank as positive sample pairs. DCL[Yeh *et al.*, 2022] removes positive sample pairs from the denominator in contrast loss to achieve positive and negative sample decoupling.

3 Method

3.1 Problem Definition

Given the model \mathcal{M}_s trained on the labeled source domain $\mathcal{D}_s = \{x_{s_i}, y_{s_i}\}_{i=1}^M$ and the unlabeled target domain $\mathcal{D}_t = \{x_{t_i}\}_{i=1}^N$, assume the feature space $\mathcal{X}_s = \mathcal{X}_t$, label space $\mathcal{Y}_s = \mathcal{Y}_t$, but marginal probability $P_s(x_s) \neq P_t(x_t)$ with conditional probability $Q(y_s | x_s) \neq Q(y_t | x_s)$. The target domain and source domain have the same C classes in this paper (known as the closed-set problem). Our method splits the model \mathcal{M}_s into two parts: a feature extractor f , and a classifier $\mathcal{C} = f(x)^T W + b$. Therefore, the output of the model is denoted as $z(x) = \delta(\mathcal{C}(f(x)))$, where δ is denoted as the softmax function.

The goal of source-free domain adaptation is to learn a feature extractor f and a classifier \mathcal{C} to predict the labels $y_t \in Y_t$ for x_t in the target domain \mathcal{D}_t . The first obstacle is that the source data are not accessible, and the second is the tremendous discrepancy between these two domains.

3.2 InfoNCE Revisit

InfoNCE is a loss function widely used for contrastive learning. It defines the augmented data of each sample i as its positive sample i^+ , and B negative sample i^- . This loss function is as follows:

$$\mathcal{L}^{\text{InfoNCE}} = \sum_{i=1}^N \log \frac{e^{z(i)^T z(i^+)/\tau}}{\sum_{b=1}^B e^{z(i)^T z(i^-)/\tau} + e^{z(i)^T z(i^+)/\tau}} \quad (1)$$

where $z(i), z(i^+)$ is called the positive pair and $z(i), z(i^-)$ is called the negative pair. $\tau \in \mathcal{R}^+$ is a scalar temperature parameter.

3.3 Motivation

Similar samples (e.g., husky and alaskan malamute) should have similar predictions, while dissimilar samples (e.g., husky and parrot) should have different predictions. Unlike the previous methods that regard an augmented sample as a positive pair, we set the neighbor samples (the top-k similar samples in the feature embedding) as positive pairs. This allows us to perform clustering directly on the data without any generative techniques, and it allows us to consider a greater number of positive pairs. The samples in the k-nearest neighbor set (measured by cosine similarity or Euclidean distance) \mathcal{K} are chosen as the positive pairs of the instance x_i , and the other samples not in this set are chosen as the negative pairs. Based on this setting, InfoNCE could expand to contain multiple positive pairs, and the loss function \mathcal{L} can be defined as follows:

$$\mathcal{L} = - \sum_{i=1}^N \sum_{j \in \mathcal{K}} \log \frac{e^{z(i)^T z(j)}}{\sum_{b \neq i, b \notin \mathcal{K}} e^{z(i)^T z(b)} + e^{z(i)^T z(j)}} \quad (2)$$

Intuitively, similar samples (e.g., husky and alaskan malamute) belong to different categories. However, the above loss function simply extends InfoNCE to multiple positive pairs, encouraging the network to classify samples with high similarity into the same category and samples with low similarity into different categories. When two categories have similar

Algorithm 1 Learning Nearest Pair Representations for SFDA

Input: Source-pretrained model \mathcal{M}_s , unlabeled target data \mathcal{D}_t .

- 1: Build three memory banks to store all the target features (\mathcal{F}) and predictions (\mathcal{P}) and the indexes of neighbors (\mathcal{N}).
- 2: Store the values of the feature bank
- 3: **while** Adaptation **do**
- 4: Sample a mini-batch \mathcal{T} from \mathcal{D}_t and update memory banks \mathcal{P} and \mathcal{F} .
- 5: For each feature in \mathcal{T} , find its K-nearest neighbors $\text{topK}(z(i))$ and update memory bank \mathcal{N} .
- 6: Retrieve and expand the neighbors from memory bank \mathcal{N} to generate W_{sim}
- 7: Compute the loss function \mathcal{L}^{CaC}
- 8: Back-propagate with the loss function and update the network parameters
- 9: **end while**
- 10: **return** solution

features, the samples are likely to be misclassified. To avoid incorrectly pulling closer to neighbors of different categories, the network needs to encourage neighbors of the same category to be closer together and neighbors of different categories to be more distant.

3.4 Contrast and Clustering

Assuming that the target feature of the source pretrained feature extractor can form clusters [Liang *et al.*, 2020; Wang *et al.*, 2022], we exploit this intrinsic ability of the pretrained model to perform SFDA by considering neighborhood information. The probability of x_i belonging to class j in C-class classification is:

$$P(Y = j | X = i) = \frac{\exp(z(i_j))}{\sum_{c=0}^{C-1} \exp(z(i_c))} \quad (3)$$

where $z(i_k) = f(x_i)^T w_k$ and it can be interpreted as the probability that instance x_i belongs to class k.

Now, we consider the following conditions. Given data x, its k-nearest neighbor set is \mathcal{K} (the method for finding the nearest k-neighbor set \mathcal{K} for each sample is described in detail in Sec.3.5), and the set \mathcal{B} denotes the other samples in the mini-batch. Intuitively, x and the neighbor set \mathcal{K} should belong to the same category, meaning that their one-hot outputs are highly consistent, so the outputs of x and its k-nearest neighbor set \mathcal{K} should be more similar to those of the k-nearest neighbor set of the other data in the current batch \mathcal{B}^k .

Therefore, we define two likelihood functions $P_{i,j}^{same}$: the probability that x_i has the same category as its neighbors, and $P_{i,j}^{dis}$: the probability that x_i has the same category as the neighbors of the other data in the current mini-batch.

$$P_{i,j}^{same} = \prod_{j \in \mathcal{K}} \frac{e^{z(i)^T z(j)}}{\sum_{q \neq i} e^{z(i)^T z(q)}} \quad (4)$$

$$P_{i,j}^{dis} = \prod_{j \in \mathcal{B}^k} \frac{e^{z(i)^T z(j)}}{\sum_{q \neq i} e^{z(i)^T z(q)}} \quad (5)$$

where \mathcal{B}^k denotes the corresponding k-nearest neighbors of \mathcal{B} . We then propose to achieve target feature clustering by minimizing the following negative logarithmic objective function, denoted as CaC:

$$\begin{aligned}\mathcal{L}^{\text{CaC}} &= -\frac{1}{N} \sum_{i=1}^N \log \frac{P_{i,j}^{\text{same}}}{P_{i,j}^{\text{dis}}} \\ &= \frac{1}{N} \sum_{i=1}^N \left(\underbrace{\sum_{j \in \mathcal{B}^k} z(i)^T z(j)}_{\text{neg:negative pairs}} - \underbrace{\sum_{j \in \mathcal{K}} z(i)^T z(j)}_{\text{pos:positive pairs}} \right) \quad (6)\end{aligned}$$

3.5 Finding the Nearest Neighbors

To retrieve the nearest neighbors for batch training, we build three memory banks: $\mathcal{F} \in \mathbb{R}^{N \times \text{Dim}}$ stores all target features, $\mathcal{P} \in \mathbb{R}^{N \times C}$ stores the corresponding prediction scores, and $\mathcal{N} \in \mathbb{R}^{N \times K}$ stores the corresponding nearest data. For two memory banks, \mathcal{F} and \mathcal{P} , which are initialized to all target features and their predictions, only the features and their predictions computed in each small batch are used to update these two repositories, as in a previous study [Liang *et al.*, 2021; Yang *et al.*, 2021].

Our work differs from previous work in that we store the indexes of the nearest neighbor samples to facilitate finding the extended neighborhoods and then use these extended neighborhoods to generate the weights W_{sim} . This step works efficiently because the memory bank \mathcal{N} is initialized to empty and is only updated after the sample similarity is computed in each mini-batch, meaning that as features are fed into the network, their corresponding nearest neighbor samples are updated in \mathcal{N} . Note that updating the nearest neighbor bank stores only the indexes¹ of the corresponding nearest neighbors, without any additional computation.

For each feature $f(i)$, its nearest neighbors, denoted as $\text{topK}(f(i))$, are the topK with the highest similarity to the memory bank \mathcal{F} and are used to compute the positive pairs in Eq.(6). The similarity between the two samples is at a maximum when the two softmax outputs have the same prediction class and are close to a one-hot vector. For the negative pair term in Eq.(6), since other samples in the mini-batch may come from the same category as $f(i)$, we claim that these similar samples should be excluded in the corresponding \mathcal{B} , because these similar samples play a relatively unimportant part in the negative pair term. To find these similar features, rather than using a larger K to find more neighbors, we utilize the expanded neighbors of each feature, i.e., the nearest neighbors of each feature and the nearest neighbors of these nearest neighbors. The feature j is regarded as a similar feature of i if $f(j) \in \text{topK}(\text{topK}(z(i)))$. For each feature in the current mini-batch, the weight $W_{\text{sim}} \in \mathbb{R}^{N \times N}$ is used to exclude those similar features. Taking the i -th feature as an example, if the j -th feature is its similar feature, then the j -th column of the i -th row in W_{sim} is 0 and the other positions are 1. Finally,

¹Each sample is given a particular index, which is the same in the dataset and the memory banks.

the objective function is denoted as:

$$\mathcal{L}^{\text{CaC}} = \frac{1}{N} \sum_{i=1}^N \left(\sum_{j \in \mathcal{B}^k} W_{\text{sim}} \cdot z(i)^T z(j) - \sum_{j \in \mathcal{K}} z(i)^T z(j) \right) \quad (7)$$

These two terms interact to achieve self-supervision of the features, where positive pairs are expected to improve the consistency of the one-hot outputs while negative pairs are expected to improve the diversity of the outputs. The weights W_{sim} are used to mine more valuable negative pairs. Our algorithm is illustrated in Algorithm 1.

4 Experiments

Datasets. We conduct the experiments on three benchmark datasets: **VisDA** is a more challenging dataset, with 12-class synthetic-to-real object recognition tasks. Its source domain consists of 152k synthetic images while the target domain contains 55k real object images. **Office-Home** contains 4 domains(Art, Clipart, Real World, Product) with 65 classes and a total of 15,500 images. **Office-31** contains 3 domains(Amazon, Webcam, DSLR) with 31 classes and 4652 images.

Evaluation. The column SF in the tables denotes source-free setting. For VisDA, we show accuracy for all classes and average over those classes (Avg in the tables). For Office-31 and Office-Home, we show the results of each task and the average accuracy over all tasks (Avg in the tables).

Baselines. We compare CaC with three types of baselines: (1) source-only: ResNet[He *et al.*, 2016]; (2) unsupervised domain adaptation with source data: DANN[Ganin *et al.*, 2016], CDAN[Long *et al.*, 2018], SRDC[Tang *et al.*, 2020], CaCo[Huang *et al.*, 2022]; and (3) source-free unsupervised domain adaptation: SHOT[Liang *et al.*, 2020], 3C-GAN[Li *et al.*, 2020], NRC[Yang *et al.*, 2021], CPGA[Qiu *et al.*, 2021], U-SFAN+[Roy *et al.*, 2022], DIPE[Wang *et al.*, 2022].

Implementation details. To ensure fair comparison with related methods, we use the same network architecture as SHOT and adopt SGD with momentum 0.9 and batch size of 64 for all datasets. Specifically, we adopt the backbone of ResNet50 for Office-Home and Office31, and ResNet101 for VisDA. The learning rate for Office-Home and Office31 is set to 1e-3 for all layers, except for the last two newly added fc layers, where we apply 1e-2. Learning rates are set 10 times smaller for VisDA. We train 15 epochs for VisDA, 40 epochs for Office-Home and 100 epochs for Office-31.

4.1 Comparison with State-of-the-Art Methods

In this section, we compare our proposed CaC with state-of-the-art methods on three DA benchmarks. In Table 1, Table 3 and Table 4, the top part shows the results for the DA methods with access to source data during adaptation. The bottom shows the results for the SFDA methods. The best results are bolded, and the second-best results are underlined.

Specifically, CaC outperforms other SOTA methods on the more challenging dataset **VisDA**, achieving the best results in various categories and ultimately obtaining excellent results,

Method	SF	VisDA												
		plane	bicycle	bus	car	horse	knife	mcycl	person	plant	sktbrd	train	truck	Avg
ResNet-101	×	55.1	53.3	61.9	59.1	80.6	17.9	79.7	31.2	81.0	26.5	73.5	8.5	52.4
DANN	×	81.9	77.7	82.8	44.3	81.2	29.5	65.1	28.6	51.9	54.6	82.8	7.8	57.4
CDAN	×	85.2	66.9	83.0	50.8	84.2	74.9	88.1	74.5	83.4	76.0	81.9	38.0	73.9
CaCo	×	90.4	80.7	78.8	57.0	88.9	87.0	81.3	79.4	88.7	88.1	86.8	63.9	80.9
SHOT	✓	94.3	88.5	80.1	57.3	93.1	94.9	80.7	80.3	91.5	89.1	86.3	58.2	82.9
3C-GAN	✓	94.8	73.4	68.8	74.8	93.1	95.4	88.6	84.7	89.1	84.7	83.5	48.1	81.6
NRC	✓	96.8	91.3	82.4	62.4	96.2	95.9	86.1	80.6	94.8	94.1	90.4	59.7	<u>85.9</u>
CPGA	✓	94.8	83.6	79.7	65.1	92.5	94.7	90.1	82.4	88.8	88.0	88.9	60.1	84.1
DIPE	✓	95.2	87.6	78.8	55.9	93.9	95.0	84.1	81.7	92.1	88.9	85.4	58.0	83.1
U-SFAN+	✓	94.9	87.4	78.0	56.4	93.8	95.1	80.5	79.9	90.1	90.1	85.3	60.4	82.7
CaC(Ours)	✓	96.9	91.0	83.3	72.3	96.9	96.1	90.7	81.6	95.1	92.9	92.0	63.2	87.7

Table 1: Accuracies (%) on VisDA(Synthesis → Real) for ResNet101-based methods.

SHOT	\mathcal{L}_{CaC}	W_{sim}	Avg
✓			82.9
	✓		87.15
	✓	✓	87.7

Table 2: Accuracy comparison with different components on VisDA

as shown in Table 1. For **Office-Home**, the proposed CaC obtains competitive results compared with other SFDA methods, as shown in Table 3. Note that our method is superior in the tasks $A \rightarrow C$, $A \rightarrow R$, $C \rightarrow R$ and $P \rightarrow C$. In addition, CaC obtains similar results to the SOTA in **Office-31**, as shown in Table 4. CaC slightly underperforms DIPE(requires a special parameter update strategy and combines five objective functions) and CPGA(epoch set to 400) on Office-Home and Office-31, but CaC achieves the best results on VisDA, far surpassing these SOTA methods. The main result is that VisDA provides sufficient data for learning positive and negative pairs so that CaC can learn better domain-invariant representations to achieve clustering of same-class samples. Moreover, CaC is able to outperform recent methods with source data (e.g., CaCo and SRDC), which demonstrates the superiority of our proposed method.

4.2 Analyzing and Ablating

Ablation study on the proposed \mathcal{L}_{CaC} and weight W_{sim}

To investigate the loss of adaptation, we show the quantitative results of the model optimized by different losses. As shown in Table 2, our proposed comparison and clustering loss \mathcal{L}_{CaC} achieves better results on VisDA than SHOT due to the pseudo-labeling that may give high confidence values for incorrect samples. Such results validate that neighbor pairs can give the network excellent self-supervised clustering ability. Moreover, we obtained the best performance when extracting more valuable negative sample pairs by using the weights W_{sim} generated from the nearest neighbors and extended neighbors.

Number of neighbors K

For the number of neighbors K used for feature clustering in Eq.(7), we show in Table 5 that our method is robust to the choice of K. From Eq.(7), we can see that K is correlated

with the sample size of the dataset, requiring a larger value on the larger VisDA dataset and a relatively smaller value for Office-Home. Additionally, the smallest dataset Office-31 is not sensitive to the size of K. As can be summarized from the results, larger K values consider more pairs, which is better for learning a robust bound. However, setting too large a K value may also include samples from other categories, bringing more noisy samples, which leads to performance degradation.

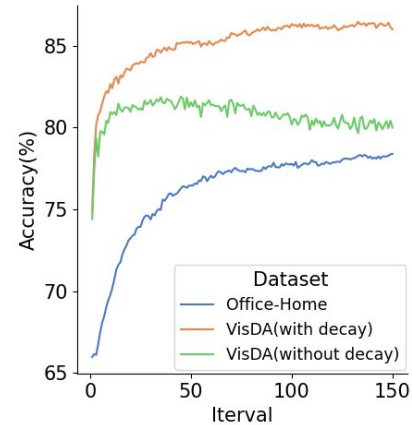


Figure 2: Accuracy of datasets.

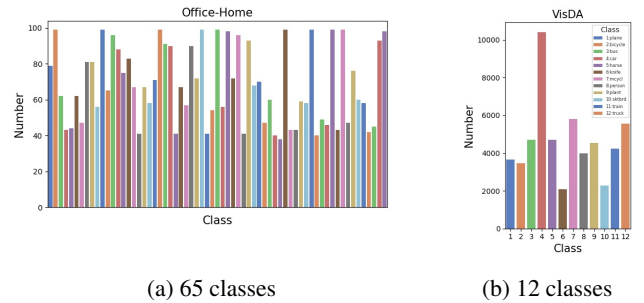


Figure 3: The proportion of classes on Office-Home and VisDA.

Method	SF	Office-Home												
		A→C	A→P	A→R	C→A	C→P	C→R	P→A	P→C	P→R	R→A	R→C	R→P	Avg
ResNet-50	×	34.9	50.0	58.0	37.4	41.9	46.2	38.5	31.2	60.4	53.9	41.2	59.9	46.1
DANN	×	45.6	59.3	70.1	47.0	58.5	60.9	46.1	43.7	68.5	63.2	51.8	76.8	57.6
CDAN	×	50.7	70.6	76.0	57.6	70.0	70.0	57.4	50.9	77.3	70.9	56.7	81.6	65.8
SRDC	×	52.3	76.3	81.0	69.5	76.2	78.0	68.7	53.8	81.7	76.3	57.1	85.0	71.3
SHOT	✓	57.1	78.1	81.5	68.0	78.2	78.1	67.4	54.9	82.2	73.3	58.8	84.3	71.8
NRC	✓	57.7	80.3	82.0	68.1	79.8	78.6	65.3	56.4	83.0	71.0	58.6	85.6	72.2
DIPE	✓	56.5	79.2	80.7	70.1	79.8	78.8	67.9	55.1	83.5	74.1	59.3	84.8	72.5
U-SFAN+	✓	57.8	77.8	81.6	67.9	77.3	79.2	67.2	54.7	81.2	73.3	60.3	83.9	71.9
CaC(Ours)	✓	59.0	79.5	82.0	67.6	79.2	79.5	66.7	56.5	81.3	74.2	58.3	84.7	<u>72.4</u>

Table 3: Accuracies (%) on Office-Home for ResNet50-based methods.

Method	SF	Office-31							Dataset	K	Avg
		A→D	A→W	D→A	D→W	W→A	W→D	Avg			
ResNet-50	×	68.9	68.4	62.5	96.7	60.7	99.3	76.1	Office-Home	1	69.79
DANN	×	82.0	96.9	99.1	79.7	68.2	67.4	82.2		3	72.16
CDAN	×	92.9	94.1	71.0	98.6	69.3	100.0	87.7		4	71.08
SRDC	×	95.8	95.7	76.7	99.2	77.1	100.0	90.8		5	70.22
CaCo	×	89.7	98.4	100.0	91.7	73.1	72.8	87.6			
SHOT	✓	94.0	90.1	74.7	98.4	74.3	99.9	88.6	Office-31	1	88.47
3C-GAN	✓	92.7	93.7	98.5	99.8	75.3	77.8	89.6		3	72.16
NRC	✓	96.0	90.8	75.3	99.0	75.0	100.0	89.4		4	89.87
CPGA	✓	94.4	94.1	98.4	99.8	76.0	76.6	<u>89.9</u>	5	89.36	
DIPE	✓	96.6	93.1	75.5	98.4	77.2	99.6	90.1	VisDA	4	85.94
U-SFAN+	✓	94.2	92.8	74.6	98.0	74.4	99.0	88.8		5	87.22
CaC(Ours)	✓	95.2	94.0	74.7	99.1	76.5	99.8	<u>89.9</u>		6	87.12
										8	85.71

Table 4: Accuracies (%) on Office-31 for ResNet50-based methods.

Table 5: Comparison in three datasets using different values of K.

Office-Home		Office31		VisDA	
β	Avg	β	Avg	β	Avg
0	72.16	0	89.73	1	82.66
0.25	72.07	0.25	89.79	5	85.74
0.5	72.00	0.5	89.78	10	87.05
0.75	71.92	0.75	89.77	15	87.44
1	71.77	1	89.80	18	87.65
2	71.26	2	89.87	20	87.2

Table 6: Comparison in three datasets using different values of β .

Interesting impact of negative pairs

We find that CaC can maintain the accuracy improvement on Office-Home, but degrades at a later stage on VisDA, as shown in the green curve in Figure 2. We first consider the class comparison of these two datasets. As shown in Figure 3, VisDA suffers from a worse class imbalance problem than Office-Home, which has a smaller number of classes and, even worse, a large gap in class proportions. Taking the fourth class of VisDA:car as an example, it is clear that a large proportion of the samples in a mini-batch belong to the car class, and the contrast loss treats the other samples in the mini-batch as potentially negative pairs. Ultimately, the network separates these samples that belong to the same class, resulting in a decrease in accuracy. As shown in Figure 4, the method is much less accurate for classes with large quantities (car, mcycl, and sktbrd) than other classes.

Dataset	Runtime(s/epoch)	Avg
SHOT	485	82.9
CaC(Ours)	471	87.7
30% for memory bank	466	87.5

Table 7: Runtime analysis of SHOT and our methods. 30% denote the percentage of target features stored in the memory bank.

Observing that sampling negative examples with truly different labels improved performance in [Chuang *et al.*, 2020], we utilized extended nearest neighbors to find more valuable negative samples; however, the contribution of the negative pair term to the loss may still be significant. Therefore, we introduce a factor $\alpha = (\frac{max_iter}{max_iter + iter})^\beta$ to control the impact of negative pairs. As the epoch time increases, the impact of the negative pairs will be reduced, where $max_iter = batch_size \times epoch$ and β controls the rate of decrease; the larger its value is, the faster the negative pair impact decreases, as shown in Table 6. The comparison results with and without decay are shown in Figure 2. After introducing the decay factor, the accuracy can be steadily improved on VisDA.

Runtime analysis

We compare the runtime in one epoch with SHOT in Table 7. For SHOT, the pseudo-label is computed by clustering in each iteration. In contrast, our nearest neighbor is a dot product operation on the features, and the nearest neighbor of

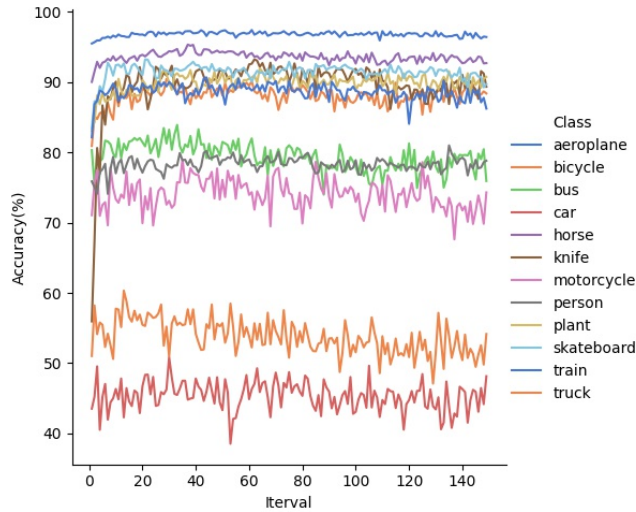


Figure 4: Accuracy of each class on VisDA.

the current sample is stored in the memory bank each time. Even though the weights W_{sim} need to use extended nearest neighbors, no additional computational consumption is required because these extended nearest neighbors can be directly retrieved from the bank. Therefore, our method can improve the performance with a relatively small amount of computation. Additionally, we reduce the size of the repository, which does not incur significant performance loss and maintains competitive results.

5 Conclusion

In this paper, we propose a source-free domain adaptation method with a self-supervised loss function that encourages one-hot output consistency with nearest neighbors to cluster of similar samples. Our method differs from previous methods in that we build an indexed memory bank for nearest neighbor samples to facilitate the retrieval of expanded neighbors, which are used to mine more valuable negative pairs without increasing the computational cost. Extensive experiments verify the importance of nearest neighbors and the impact of negative pairs, as well as proving that the proposed method outperforms other state-of-the-art source-free domain adaptation methods on several benchmarks.

References

[Chen *et al.*, 2020] Ting Chen, Simon Kornblith, Mohammad Norouzi, and Geoffrey Hinton. A simple framework for contrastive learning of visual representations. In *International conference on machine learning*, pages 1597–1607, 2020.

[Chuang *et al.*, 2020] Ching-Yao Chuang, Joshua Robinson, Yen-Chen Lin, Antonio Torralba, and Stefanie Jegelka. De-biased contrastive learning. *Advances in neural information processing systems*, 33:8765–8775, 2020.

[Dwibedi *et al.*, 2021] Debidatta Dwibedi, Yusuf Aytar, Jonathan Tompson, Pierre Sermanet, and Andrew Zisser-

man. With a little help from my friends: Nearest-neighbor contrastive learning of visual representations. In *Proceedings of the IEEE/CVF International Conference on Computer Vision*, pages 9588–9597, 2021.

- [Ganin *et al.*, 2016] Yaroslav Ganin, Evgeniya Ustinova, Hana Ajakan, Pascal Germain, Hugo Larochelle, François Laviolette, Mario Marchand, and Victor Lempitsky. Domain-adversarial training of neural networks. *The journal of machine learning research*, 17(1):2096–2030, 2016.
- [He *et al.*, 2016] Kaiming He, Xiangyu Zhang, Shaoqing Ren, and Jian Sun. Deep residual learning for image recognition. In *Proceedings of the IEEE conference on computer vision and pattern recognition*, pages 770–778, 2016.
- [He *et al.*, 2020] Kaiming He, Haoqi Fan, Yuxin Wu, Saining Xie, and Ross Girshick. Momentum contrast for unsupervised visual representation learning. In *Proceedings of the IEEE/CVF conference on computer vision and pattern recognition*, pages 9729–9738, 2020.
- [Hou and Zheng, 2021] Yunzhong Hou and Liang Zheng. Visualizing adapted knowledge in domain transfer. In *Proceedings of the IEEE/CVF Conference on Computer Vision and Pattern Recognition*, pages 13824–13833, 2021.
- [Huang *et al.*, 2022] Jiaxing Huang, Dayan Guan, Aoran Xiao, Shijian Lu, and Ling Shao. Category contrast for unsupervised domain adaptation in visual tasks. In *Proceedings of the IEEE/CVF Conference on Computer Vision and Pattern Recognition*, pages 1203–1214, 2022.
- [Kalantidis *et al.*, 2020] Yannis Kalantidis, Mert Bulent Sariyildiz, Noe Pion, Philippe Weinzaepfel, and Diane Larlus. Hard negative mixing for contrastive learning. *Advances in Neural Information Processing Systems*, 33:21798–21809, 2020.
- [Kundu *et al.*, 2020] Jogendra Nath Kundu, Naveen Venkat, R Venkatesh Babu, et al. Universal source-free domain adaptation. In *Proceedings of the IEEE/CVF Conference on Computer Vision and Pattern Recognition*, pages 4544–4553, 2020.
- [Kundu *et al.*, 2022] Jogendra Nath Kundu, Akshay R Kulkarni, Suvaansh Bhambri, Deepesh Mehta, Shreyas Anand Kulkarni, Varun Jampani, and Venkatesh Babu Radhakrishnan. Balancing discriminability and transferability for source-free domain adaptation. In *International Conference on Machine Learning*, pages 11710–11728. PMLR, 2022.
- [Lee *et al.*, 2022] Jonghyun Lee, Dahyun Jung, Junho Yim, and Sungroh Yoon. Confidence score for source-free unsupervised domain adaptation. In *International Conference on Machine Learning*, pages 12365–12377. PMLR, 2022.
- [Li *et al.*, 2020] Rui Li, Qianfen Jiao, Wenming Cao, Hui San Wong, and Si Wu. Model adaptation: Unsupervised domain adaptation without source data. In *Proceedings of the IEEE/CVF Conference on Computer Vision and Pattern Recognition*, pages 9641–9650, 2020.
- [Liang *et al.*, 2020] Jian Liang, Dapeng Hu, and Jiashi Feng. Do we really need to access the source data? source hypothesis transfer for unsupervised domain adaptation. In *In-*

- ternational Conference on Machine Learning, pages 6028–6039. PMLR, 2020.
- [Liang *et al.*, 2021] Jian Liang, Dapeng Hu, and Jiashi Feng. Domain adaptation with auxiliary target domain-oriented classifier. In *Proceedings of the IEEE/CVF Conference on Computer Vision and Pattern Recognition*, pages 16632–16642, 2021.
- [Lin *et al.*, 2022] Kun-Yu Lin, Jiaming Zhou, Yukun Qiu, and Wei-Shi Zheng. Adversarial partial domain adaptation by cycle inconsistency. In *European Conference on Computer Vision*, pages 530–548. Springer, 2022.
- [Long *et al.*, 2018] Mingsheng Long, Zhangjie Cao, Jianmin Wang, and Michael I Jordan. Conditional adversarial domain adaptation. *Advances in neural information processing systems*, 31, 2018.
- [Mitrovic *et al.*, 2020] Jovana Mitrovic, Brian McWilliams, and Melanie Rey. Less can be more in contrastive learning. In *Proceedings on "I Can't Believe It's Not Better!" at NeurIPS Workshops*, volume 137, pages 70–75. PMLR, 2020.
- [Oord *et al.*, 2018] Aaron van den Oord, Yazhe Li, and Oriol Vinyals. Representation learning with contrastive predictive coding. *arXiv preprint arXiv:1807.03748*, 2018.
- [Qiu *et al.*, 2021] Zhen Qiu, Yifan Zhang, Hongbin Lin, Shuaicheng Niu, Yanxia Liu, Qing Du, and Mingkui Tan. Source-free domain adaptation via avatar prototype generation and adaptation. In *Proceedings of the Thirtieth International Joint Conference on Artificial Intelligence*, pages 2921–2927, Montreal, Canada, 19–27 August 2021. ijcai.org.
- [Roy *et al.*, 2022] Subhankar Roy, Martin Trapp, Andrea Pilzer, Juho Kannala, Nicu Sebe, Elisa Ricci, and Arno Solin. Uncertainty-guided source-free domain adaptation. In *European Conference on Computer Vision*, pages 537–555. Springer, 2022.
- [Tang *et al.*, 2020] Hui Tang, Ke Chen, and Kui Jia. Unsupervised domain adaptation via structurally regularized deep clustering. In *Proceedings of the IEEE/CVF conference on computer vision and pattern recognition*, pages 8725–8735, 2020.
- [Tian *et al.*, 2020] Yonglong Tian, Dilip Krishnan, and Phillip Isola. Contrastive multiview coding. In *European conference on computer vision*, pages 776–794, 2020.
- [Wang *et al.*, 2022] Fan Wang, Zhongyi Han, Yongshun Gong, and Yilong Yin. Exploring domain-invariant parameters for source free domain adaptation. In *Proceedings of the IEEE/CVF Conference on Computer Vision and Pattern Recognition*, pages 7151–7160, 2022.
- [Xia *et al.*, 2021] Haifeng Xia, Handong Zhao, and Zhengming Ding. Adaptive adversarial network for source-free domain adaptation. In *Proceedings of the IEEE/CVF International Conference on Computer Vision*, pages 9010–9019, 2021.
- [Yang *et al.*, 2021] Shiqi Yang, Joost van de Weijer, Luis Herranz, Shangling Jui, et al. Exploiting the intrinsic neighborhood structure for source-free domain adaptation. *Advances in Neural Information Processing Systems*, 34:29393–29405, 2021.
- [Ye *et al.*, 2019] Mang Ye, Xu Zhang, Pong C Yuen, and Shih-Fu Chang. Unsupervised embedding learning via invariant and spreading instance feature. In *Proceedings of the IEEE/CVF Conference on Computer Vision and Pattern Recognition*, pages 6210–6219, 2019.
- [Yeh *et al.*, 2022] Chun-Hsiao Yeh, Cheng-Yao Hong, Yen-Chi Hsu, Tyng-Luh Liu, Yubei Chen, and Yann LeCun. Decoupled contrastive learning. In *European Conference on Computer Vision*, pages 668–684. Springer, 2022.
- [You *et al.*, 2019] Kaichao You, Mingsheng Long, Zhangjie Cao, Jianmin Wang, and Michael I Jordan. Universal domain adaptation. In *Proceedings of the IEEE/CVF conference on computer vision and pattern recognition*, pages 2720–2729, 2019.